

Actin reorganization as the molecular basis for the regulation of apoptosis in gastrointestinal epithelial cells

Y Wang^{1,4}, SP George^{2,4}, K Srinivasan³, S Patnaik² and S Khurana^{*2}

The gastrointestinal (GI) epithelium is a rapidly renewing tissue in which apoptosis represents part of the overall homeostatic process. Regulation of apoptosis in the GI epithelium is complex with a precise relationship between cell position and apoptosis. Apoptosis occurs spontaneously and in response to radiation and cytotoxic drugs at the base of the crypts. By contrast, the villus epithelial cells are extremely resistant to apoptosis. The molecular mechanism underlying this loss of function of villus epithelial cells to undergo apoptosis shortly after their exit from the crypt is unknown. In this study we demonstrate for the first time, that deletion of two homologous actin-binding proteins, villin and gelsolin renders villus epithelial cells extremely sensitive to apoptosis. Ultrastructural analysis of the villin-gelsolin^{-/-} double-knockout mice shows an abnormal accumulation of damaged mitochondria demonstrating that villin and gelsolin function on an early step in the apoptotic signaling at the level of the mitochondria. A characterization of functional and ligand-binding mutants demonstrate that regulated changes in actin dynamics determined by the actin severing activities of villin and gelsolin are required to maintain cellular homeostasis. Our study provides a molecular basis for the regulation of apoptosis in the GI epithelium and identifies cell biological mechanisms that couple changes in actin dynamics to apoptotic cell death.

Cell Death and Differentiation (2012) 19, 1514–1524; doi:10.1038/cdd.2012.28; published online 16 March 2012

The gastrointestinal (GI) epithelium is characterized by a very high cellular turnover rate, which leads to renewal of the intestinal epithelium every 3–5 days.¹ Apoptosis is a key regulator of this normal turnover.¹ Abnormalities associated with apoptosis in the epithelium have been linked to most major GI disorders, including ischemia reperfusion injury, graft-*versus*-host disease, inflammatory bowel disease, necrotizing enterocolitis, celiac disease, GI infections and colorectal cancer.^{2–4} A very intriguing feature of apoptosis in the intestine is that post-mitotic epithelial cells that migrate out of the crypts and move up the villi rapidly lose their ability to undergo apoptosis.⁵ The molecular mechanism responsible for the acquisition of this highly resistant phenotype of the villus cells within a few hours of their exit from the crypts has been perplexing and has remained unidentified. Characterization of this apoptosis-resistant phenotype of the villus cell could identify abnormalities in apoptosis that initiate colorectal cancer and its resistance to chemotherapeutic drugs and radiotherapy.²

Radiation therapy is an established treatment for both primary and recurrent abdominal malignancies, including

colorectal, urological, and gynecological cancers. However, a major side effect of radiation therapy is radiation enteropathy that is characterized by loss of the epithelial barrier, mucosal inflammation and progressive fibrosis, which can lead ultimately to organ failure. Radiation enteropathy develops exclusively as a result of crypt cell death.⁶ There is currently no effective treatment or preventive approach for this unwanted enteropathy. A better understanding of the apoptosis-resistant phenotype of the villus cell could provide an endogenous mechanism to sustain mucosal integrity, modulate vulnerability to cytotoxic injury and, modulate the reparative response of the GI epithelium during radiation therapy.⁷

Villin and gelsolin belong to a family of actin-binding proteins that share significant structural and functional homology.⁸ Both proteins share six repeated domains with very similar ligand-binding sites for G-actin, F-actin and phosphatidylinositol 4,5-bisphosphate (PIP₂).⁸ Both proteins sever, cap and nucleate actin filaments and similar to villin, gelsolin is expressed in very significant amounts in the intestine where it localizes to the apical surface of

¹The Department of Physiology, The University of Tennessee Health Science Center, Memphis, TN 38163, USA; ²The Department of Biology and Biochemistry, The University of Houston, Houston, TX 77204-5001, USA and ³The Department of Biological Sciences, Vanderbilt University, Nashville, TN 37232, USA

*Corresponding author: S Khurana, Department of Biology and Biochemistry, The University of Houston, 369 Science and Research Building 2, Houston, TX 77204-5001, USA. Tel: + 713 743 2705; Fax: + 713 743 2636; E-mail: skhurana@uh.edu

⁴These authors contributed equally to this work.

Keywords: villin; gelsolin; severing; apoptosis; intestine

Abbreviations: MDCK, Madin–Darby canine kidney epithelial cell line; VIL/WT, MDCK Tet-Off cells stably expressing wild-type villin; CPT, camptothecin; GSN/WT, MDCK Tet-Off cells stably expressing wild-type gelsolin; GI, gastrointestinal; PP2, 4-amino-5-(4-chlorophenyl)-7-(*t*-butyl)pyrazolo[3,4-*d*]pyrimidine; DKO, villin/gelsolin double-knockout mice; LDH, lactate dehydrogenase; ALT, alanine aminotransferase; SGPT, serum glutamic pyruvic transaminase; SEYFP, super enhanced yellow fluorescent protein

Received 24.10.11; revised 26.1.12; accepted 08.2.12; Edited by JA Cidlowski; published online 16.3.12

enterocytes.⁹ In this study we describe a fortuitous observation, that deletion of villin and gelsolin renders villus epithelial cells like the crypt epithelial cells, extremely sensitive to both 'spontaneous' and 'radiation-induced' apoptosis. Our study elucidates a new molecular mechanism of apoptosis in the GI epithelium and identifies the complex connections between the hierarchies to undergo apoptotic cell death along the crypt-villus axis. Our study demonstrates that a threshold of dynamic actin is crucial for cellular homeostasis. To the best of our knowledge, this is the first demonstration of any 'endogenous' protein regulating apoptosis in the villus epithelial cells. The novelty of our observation allows us to also identify the complex cellular and molecular mechanisms regulated by villin and gelsolin to modify the apoptotic response of the GI epithelium that could provide a molecular basis for the etiopathogenesis of many GI diseases.

Results

Villin inhibits apoptosis by preserving actin dynamics.

We have previously shown that villin is a key regulator of apoptosis in the GI epithelium.¹⁰ In eukaryotic cells, changes in total cellular actin have been linked to apoptotic cell death.¹¹ Hence, we hypothesized, that villin could inhibit apoptosis by preventing the accumulation of F-actin. To test this hypothesis, we used Madin–Darby canine kidney epithelial cell line (MDCK) Tet-Off cells stably transfected with human villin, cultured in the absence (VIL/WT) or presence (VIL/NULL) of doxycycline. Total cellular F- and G-actin content of VIL/NULL and VIL/WT cells treated without or with camptothecin (CPT, 20 μ M, 5 h, 37°C) was measured as described by us previously.¹⁰ The levels of filamentous actin were similar in untreated VIL/NULL and VIL/WT cells, although VIL/WT cells showed a reorganization of F-actin consistent with previous reports that expression of villin results in the loss of stress fibers and redistribution of F-actin (Figure 1a).¹² Following exposure to CPT the levels of F-actin were significantly increased in VIL/NULL cells (* $P < 0.001$ compared with VIL/NULL cells in the absence of CPT and # $P < 0.001$ compared with VIL/WT cells; $n = 6$). In contrast, VIL/WT cells showed no significant changes in total F-actin levels following CPT treatments, indicating that villin prevents CPT-induced accumulation of F-actin. Flow cytometric analysis revealed an increase in the total F- and a decrease in the total G-actin content in VIL/NULL cells following CPT treatment (Figure 1b, Supplementary Figure 1A). In contrast, CPT-treated VIL/WT cells maintained their cellular G- and F-actin levels similar to untreated control cells (Figure 1b, Supplementary Figure 1A). Consistent with that, VIL/WT cells had higher levels of free barbed ends compared with VIL/NULL cells ($P < 0.05$, $n = 3$; Figure 1c). In response to CPT, the number of free barbed ends in VIL/NULL cells decreased significantly, ($P < 0.01$, $n = 3$). Following CPT treatment, the number of free barbed ends in VIL/WT cells increased quite significantly ($P < 0.01$, $n = 3$) indicating increased actin severing. These results reveal that the susceptibility of epithelial cells to undergo apoptosis correlates with changes in total cellular F-actin levels.

Furthermore, the ability of villin to sever actin and maintain steady-state actin dynamics appears to contribute to its anti-apoptotic function.

The actin-severing activity of villin is required for its anti-apoptotic function.

On the basis of the studies done in yeast, plant and mammalian cells, two models have been proposed to describe the regulation of apoptosis by the microfilament structure. The first predicts that actin stabilization promotes apoptosis.¹³ The second predicts that the PIP₂ binding activity of actin-regulatory proteins influences the execution phase of apoptosis.¹⁴ Villin is an actin-severing protein that binds PIP₂.⁸ To identify the molecular mechanism by which villin modifies GI homeostasis, wild-type and mutant villin proteins that either lack the actin-severing domain (PB2) or lack each of the three identified PIP₂ binding domains of villin (PB1, PB2 or PB5) were characterized for their anti-apoptotic function. These mutants were constructed and expressed in MDCK cells as summarized in Supplementary Figure 2. Functional characterization of these mutants, including their effect on actin kinetics have been described in our previous studies.¹⁵ PB2 represents an overlapping PIP₂ and F-actin side-binding site that regulates actin severing by villin.¹⁶ Mutation of three basic residues R138A, K145A and R146A (VIL/RKR) within the PB2 domain of villin also results in the complete loss of actin severing by villin and PIP₂ binding by this domain of villin.^{15,16} To distinguish between the overlapping PIP₂ and actin-severing functions of villin domain PB2, we generated an additional mutant VIL/R138A. We have previously shown that mutation of this single residue, R138 within the PB2 domain of villin (R138A) results in significant (~85%) loss of PIP₂ binding by this site.¹⁵ However, mutation of R138 (R138A) has a negligible effect on the actin-severing activity of villin.¹⁶ Consistent with our previous findings, a significant increase in the number of apoptotic VIL/NULL cells was noted 5 h post-CPT treatment, whereas no significant change in cell death was noted in VIL/WT cells (Figure 2a, Supplementary Figure 1B).¹⁰ Deletion of the PIP₂ binding sites PB1 and PB5 had no significant effect on cell viability. In contrast, VIL/ Δ PB2 and VIL/RKR showed a significant increase in DNA fragmentation and a comparable increase in propidium iodide (PI) positive cells (asterisk denotes $P < 0.01$, $n = 6$). However, the villin mutant VIL/R138A showed no significant change in the number of apoptotic cells compared with VIL/WT cells. In keeping with these data there was a significant inhibition of executor caspase-3 in cells expressing full-length villin, PB1, PB5 and R138A, whereas VIL/NULL and cells expressing villin mutants PB2 and RKR showed a significant increase in the caspase-3 activity as early as 4 h post-treatment (asterisk denotes $P < 0.01$, $n = 6$ compared with VIL/NULL cells; Figure 2b). Together these data demonstrate that the actin-severing activity of villin is required for its anti-apoptotic function.

Gelsolin inhibits apoptosis by preserving actin dynamics.

Gelsolin is the closest homolog of villin and it exhibits remarkable homology to villin in a region where the actin-severing activity of both proteins resides.¹⁷ To determine whether actin severing is a conserved regulatory pathway to

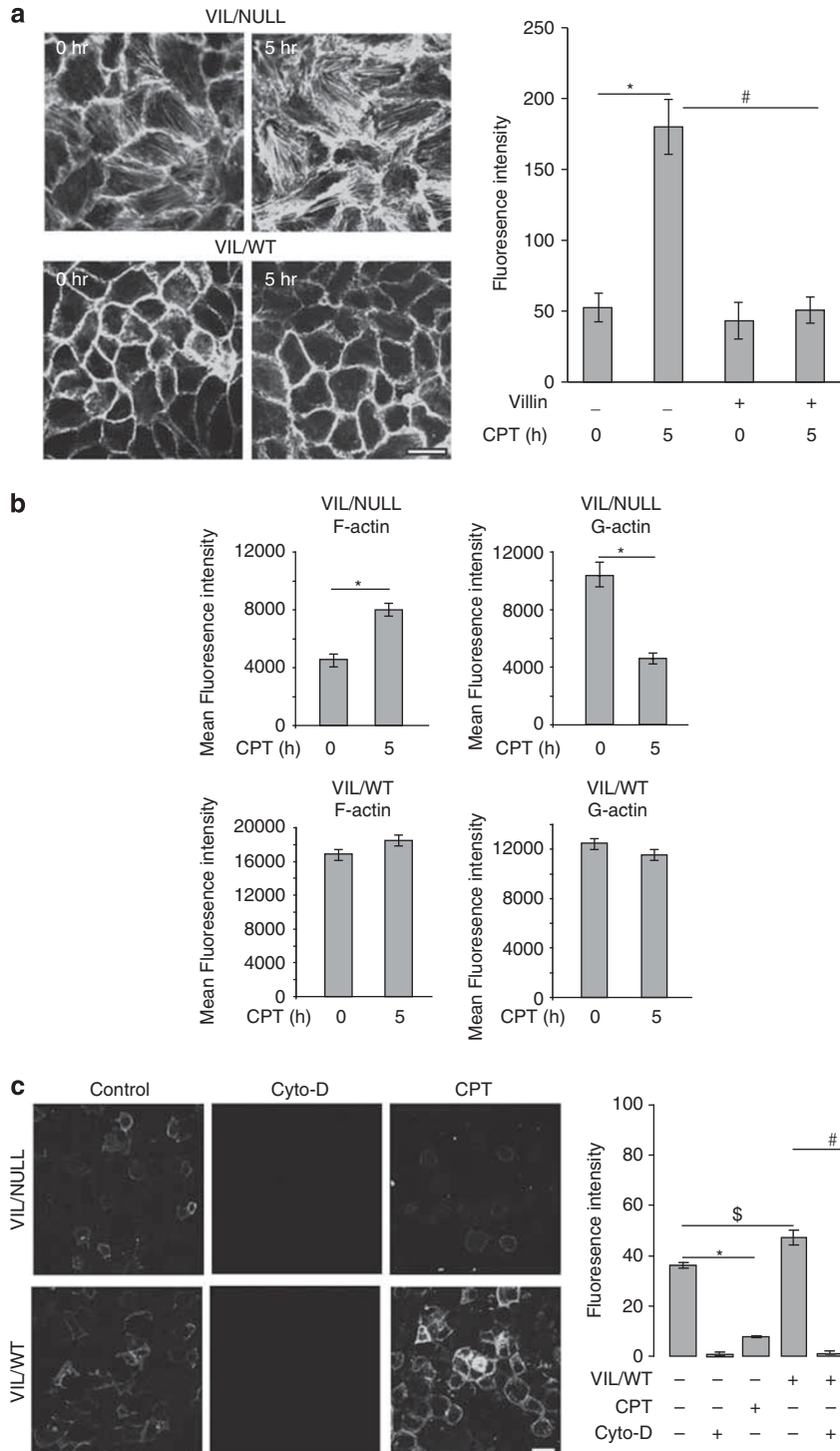


Figure 1 Actin severing by villin is required to maintain intracellular actin dynamics in response to CPT treatment. **(a)** F-actin levels in VIL/NULL and VIL/WT cells treated with CPT (20 μ M, 0–5 h). CPT treatment significantly increased total cellular F-actin concentration in VIL/NULL cells ($*P < 0.001$, $n = 6$). F-actin concentrations in CPT-treated VIL/NULL cells were significantly higher than F-actin in CPT-treated VIL/WT cells ($#P < 0.001$, $n = 6$). Bar, 20 μ m. **(b)** Total cellular F- and G-actin levels were measured in VIL/NULL and VIL/WT cells treated with CPT (20 μ M, 0–5 h). Experiments were performed in triplicate. In response to CPT treatment there was a significant increase in F-actin ($*P < 0.01$, $n = 3$) and decrease in G-actin ($*P < 0.001$, $n = 3$) levels in VIL/NULL cells. **(c)** Free barbed ends were visualized as described in Materials and Methods. Alexa 488-labeled actin incorporation was measured using confocal laser scanning microscopy. Experiments were performed in triplicate. Cytochalasin D that binds to the barbed ends of actin filaments was used as a control. Untreated VIL/WT cells had significantly higher numbers of free barbed ends compared with untreated VIL/NULL cells ($#P < 0.05$, $n = 3$). CPT treatment increased the number of free barbed ends in VIL/WT cells compared with untreated VIL/WT cells ($#P < 0.01$, $n = 3$). In contrast CPT treatment significantly reduced the number of free barbed ends in VIL/NULL cells compared with untreated VIL/NULL cells ($*P < 0.01$, $n = 3$). Bar, 20 μ m

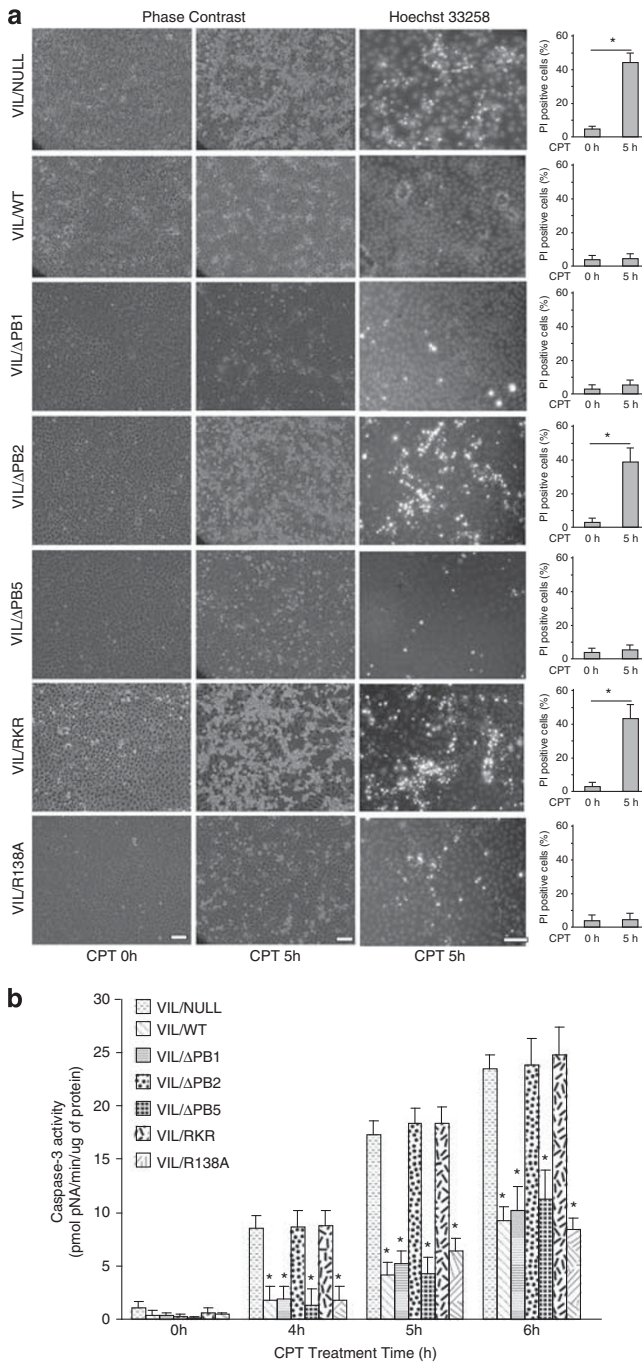


Figure 2 Actin depolymerization by villin is required for its anti-apoptotic function. MDCK Tet-Off cells expressing full-length and mutant villin proteins were cultured in the presence (VIL/NULL) or absence of doxycycline and treated with CPT (20 μ M, 0–5 h). **(a)** VIL/NULL- and villin-expressing cells were visualized by phase contrast microscopy and stained with Hoechst 33258 to identify apoptotic cells. This is representative of six other experiments with similar data. Bar, 50 μ m. PI permeability was analyzed by flow cytometry as a quantitative measure of cell viability. There was a significant increase in PI positive VIL/NULL, VIL/ΔPB2 and VIL/RKR cells in response to CPT treatment ($*P < 0.01$, $n = 9$). **(b)** Caspase-3 activity was measured in MDCK Tet-Off VIL/NULL- and villin-expressing (wild-type and mutant) cells treated without or with CPT (20 μ M) for 0–6 h. Caspase-3 activity was significantly inhibited in VIL/WT, VIL/ΔPB1, VIL/ΔPB5 and VIL/R138A cells as early as 4 h post treatment ($*P < 0.01$, $n = 6$)

inhibit apoptosis and maintain GI homeostasis, we elected to study the effects of gelsolin on cellular actin dynamics. Consistent with our findings with VIL/WT cells, expression of gelsolin protected cells from CPT-induced apoptosis, confirming the role of gelsolin as an anti-apoptotic protein (Figures 3a and b; Supplementary Figure 1C). MDCK Tet-Off cells stably transfected with human cytoplasmic gelsolin cultured in the absence (GSN/WT) or presence (GSN/NULL) of doxycycline were used for these studies. A quantitative measure of total cellular G- and F-actin levels in cells expressing human cytoplasmic gelsolin confirmed that like villin, gelsolin preserved cellular actin dynamics to prevent apoptotic cell death (Figure 3c; Supplementary Figure 1D). Similar to VIL/WT cells, GSN/WT cells also showed higher actin filament severing activity with a significant increase in the number of free barbed ends in response to CPT treatment (Figure 3d). Together, these data make a case for the presence of a conserved actin-cytoskeleton mediated mechanism that underpins the regulation of apoptosis in GI epithelial cells.

Regulated actin severing inhibits apoptosis. Remodeling the actin cytoskeleton in response to stress is a fundamental process in eukaryotic cells. Our data demonstrate that actin severing by villin and gelsolin prevents apoptosis. On the basis of that we asked if global changes in total cellular F-actin can prevent cell death. We tested the effects of the actin depolymerizing drug latrunculin on CPT-induced apoptosis in VIL/NULL and VIL/WT cells. Dose–response studies were done to identify appropriate concentration of drugs to depolymerize or stabilize actin (Supplementary Figure 3). Treatment of VIL/NULL cells with latrunculin did not prevent apoptosis (Supplementary Figure 4A). More surprisingly, pre-treatment of CPT-treated VIL/WT cells with latrunculin induced apoptosis in cells that were otherwise resistant to CPT-induced apoptosis (Supplementary Figure 4B). These findings indicated to us that maintaining a threshold of dynamic actin rather than actin severing *per se* was crucial for cellular homeostasis.

Villin is tyrosine-phosphorylated both *in vitro* and *in vivo* and tyrosine phosphorylation of villin enhances its actin-severing function.¹⁸ We have previously identified 10 phosphorylation sites in villin and demonstrated that mutation of these sites inhibits the actin severing activity of villin.¹⁹ Further, we have demonstrated the absolute requirement of c-Src kinase for tyrosine phosphorylation of villin.²⁰ Gelsolin is also tyrosine-phosphorylated by c-Src kinase, although the tyrosine-phosphorylated residues and the significance of phosphorylation for the actin-regulatory functions of gelsolin have not been identified.²¹ To characterize the significance of tyrosine-phosphorylated villin in the regulation of epithelial cell viability, we elected to use the pharmacological inhibitor of c-Src kinase, PP2 (10 μ M) and its negative control PP3 (10 μ M), as well as the mutant villin protein that lacks the tyrosine phosphorylation sites (VIL/AYFM).¹⁹ VIL/AYFM is not tyrosine-phosphorylated *in vitro* or in MDCK cells.¹⁹ As shown in Figure 4a, villin is tyrosine-phosphorylated in response to CPT treatment. Pre-treatment of VIL/WT cells with PP2 (10 μ M) reversed the anti-apoptotic effects of villin (Figure 4b; Supplementary Figure 1E). PP2 by itself had no effect on

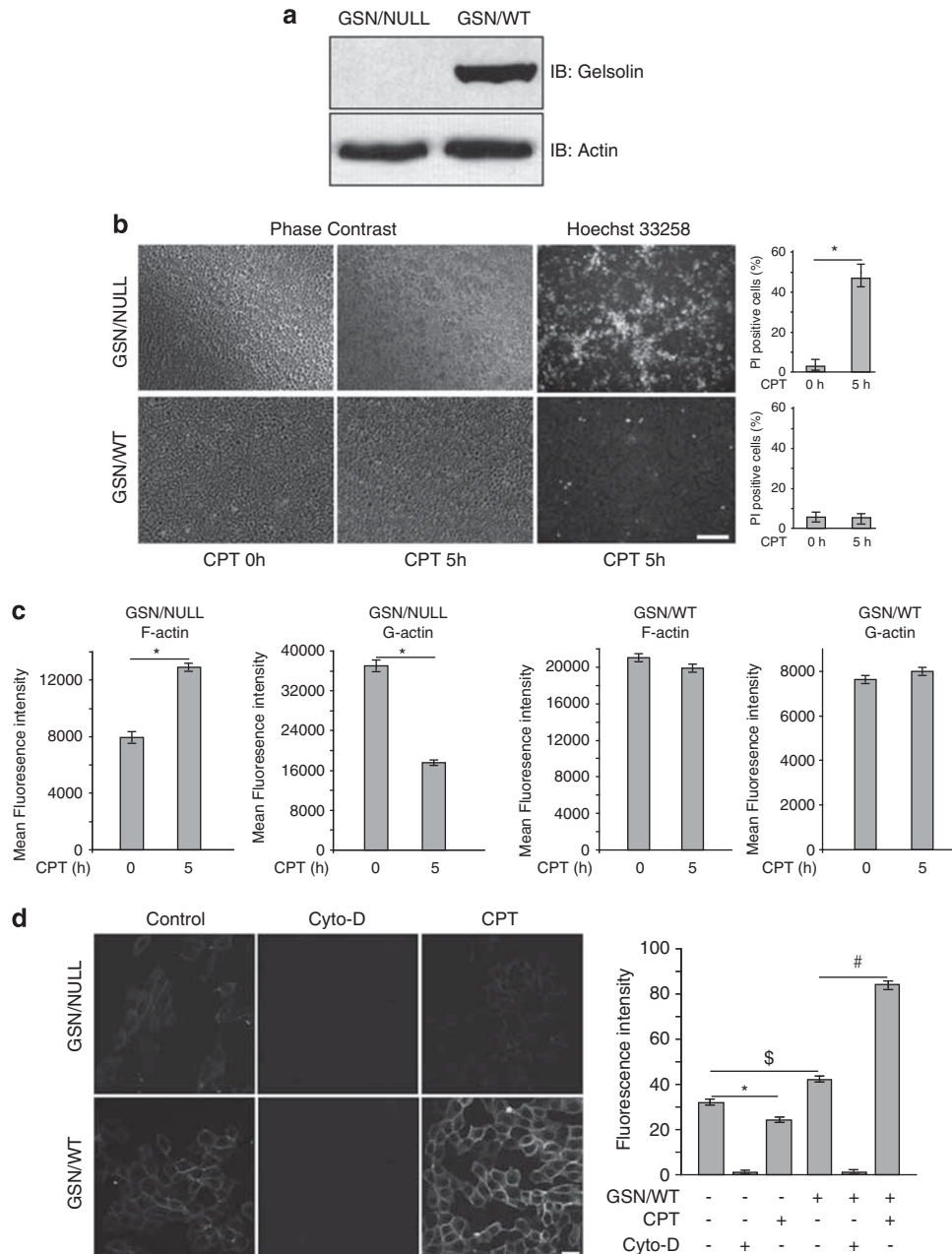


Figure 3 Actin severing by gelsolin is required to maintain intracellular actin dynamics in response to CPT treatment. **(a)** Western analysis of full-length human cytoplasmic gelsolin expressed in MDCK Tet-Off cells. Western blot with anti-actin antibody was performed in parallel as a quantitative control. Data are representative of six experiments with similar results. **(b)** GSN/NULL and GSN/WT cells were treated with CPT (20 μ M, 0–5 h) and apoptosis measured as described in the Methods. Apoptotic cells were visualized by phase-contrast microscopy and identified using Hoechst 33258 staining. All experiments were performed in triplicate, with similar results, $n = 6$. Bar, 50 μ m. PI permeability was analyzed by flow cytometry as a quantitative measure of cell viability. There was a significant increase in PI positive GSN/NULL cells in response to CPT treatment ($*P < 0.01$, $n = 6$). **(c)** Total cellular F- and G-actin levels were measured in GSN/WT cells treated with CPT (20 μ M, 0–5 h). There was a significant increase in F-actin ($*P < 0.01$, $n = 3$) and decrease in G-actin ($*P < 0.01$, $n = 3$) in GSN/NULL cells in response to CPT treatment. Experiments were performed in triplicate. **(d)** Free barbed ends were localized as described in Methods. Alexa 488-labeled actin incorporation was assessed by confocal laser scanning microscopy. Experiments were performed in triplicate. Untreated GSN/WT cells had significantly higher numbers of free barbed ends compared with GSN/NULL cells ($^{\#}P < 0.05$, $n = 3$). CPT treatment increased the number of free barbed ends in GSN/WT cells compared with untreated GSN/WT cells ($^{\#}P < 0.01$, $n = 3$). In contrast CPT treatment reduced the number of free barbed ends in GSN/NULL cells compared with untreated GSN/NULL cells ($*P < 0.05$, $n = 3$). Cytochalasin D prevented the incorporation of Alexa 488-labeled actin into both GSN/NULL and GSN/WT cells. Bar, 20 μ m

the actin cytoskeleton (data not shown). We have previously shown that PP2 prevents the tyrosine phosphorylation of villin.²² Cells expressing VIL/AYFM showed a significant increase in the number of apoptotic cells in response to CPT

treatment (Figure 4c; Supplementary Figure 1F). In agreement with these data, there was a significant increase in the caspase-3 activity in VIL/NULL and VIL/AYFM cells but not in cells expressing full-length villin ($P < 0.01$, $n = 6$; Figure 4d).

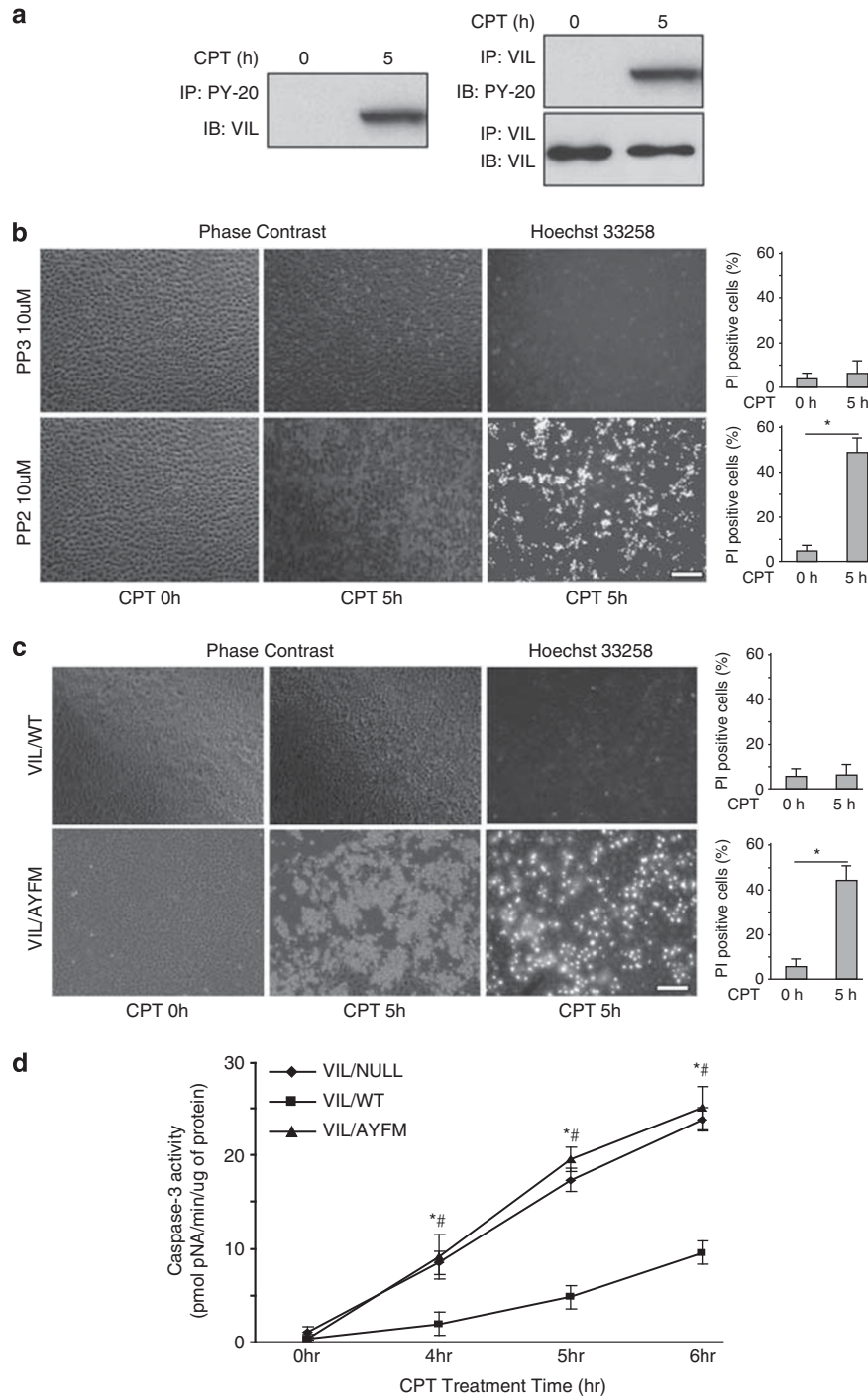


Figure 4 Regulated actin-severing function of villin is required for its anti-apoptotic function. **(a)** Villin is tyrosine-phosphorylated in CPT-treated MDCK cells. Tyrosine-phosphorylated villin was identified by immunoprecipitation (IP) of villin and immunoblot (IB) analysis with phosphotyrosine antibody (PY-20) and *vice versa*. The immunoblot was re-probed with anti-villin antibody. Data are representative of four experiments with similar results. **(b)** Inhibiting tyrosine phosphorylation of villin with the Src kinase inhibitor PP2 (10 μ M) reverses the anti-apoptotic function of villin. The negative control PP3 (10 μ M) had no effect on apoptosis in VIL/WT cells). Apoptotic cells were visualized by phase-contrast microscopy and identified using Hoechst 33258 staining. All experiments were performed in triplicate, with similar results. Bar, 50 μ m. PI positive cells were identified by flow cytometry. There was a significant increase ($*P < 0.01$, $n = 9$) in PI positive VIL/WT pre-treated with the Src kinase inhibitor PP2. **(c)** MDCK Tet-Off cells expressing the phosphorylation site mutant of villin, VIL/AYFM failed to inhibit CPT-induced apoptosis. Apoptotic cells were visualized in VIL/WT and VIL/AYFM cells by phase-contrast microscopy and identified using Hoechst 33258 staining. All experiments were performed in triplicate, with similar results, $n = 6$. Bar, 50 μ m. PI positive cells were identified by flow cytometry. There was a significant increase in the number of PI positive VIL/AYFM cells in response to CPT treatment ($*P < 0.01$, $n = 9$). **(d)** Caspase-3 activity was significantly inhibited in VIL/NULL and VIL/AYFM cells between 4–6 hours post-treatment ($*AYFM$ compared with VIL/WT cells; $^{\#}NULL$ cells compared with VIL/WT; $P < 0.01$, $n = 6$)

As the PIP₂ and F-actin binding sites within PB2 are overlapping in villin and gelsolin, the tyrosine phosphorylation site mutant also provides independent validation of the significance of actin severing for villin's anti-apoptotic function. Thus, the anti-apoptotic function of villin is lost if the actin-severing activity of villin is inhibited either by deletion of the F-actin side-binding and severing domain (VIL/ Δ PB2, VIL/RKR) or by mutation of the phosphorylation sites (VIL/AYFM). Pre-treatment of GSN/WT cells with PP2 (10 μ M) likewise reversed the anti-apoptotic effects of gelsolin (Supplementary Figure 5). We suggest that phosphorylation of villin and gelsolin could provide a molecular basis to regulate apoptosis in the GI epithelium that could be used as a therapeutic target to modify apoptosis in the GI epithelium.²³ Our mutational studies were limited to villin as similar mutants have not yet been characterized for gelsolin.

Villin and gelsolin regulate 'spontaneous' and 'stimulated' apoptosis in the intestinal villus cells. On the basis of the overlapping functions of villin and gelsolin in the regulation of apoptosis, we elected to examine the effect of deleting both these actin-severing proteins from the GI epithelium. The specific function of gelsolin in the GI epithelium and the functional redundancy and compensatory expression of villin and gelsolin in GI epithelial cells has never been addressed previously. To understand the functions of these closely related actin-severing proteins we created the villin/gelsolin^{-/-} double-knockout mice (DKO). The DKO mice were genotyped by PCR and verified by immunohistochemistry (Supplementary Figure 6). Several phenotypic changes were identified within the DKO colony housed in conventional, specific pathogen-free conditions. Blood biochemistry was performed on eight DKO and eight WT littermates at 10 weeks of age, using a commercial facility (Anl Lytics, Inc. Gaithersburg, MD, USA) that showed significantly higher levels of lactate dehydrogenase (twofold increase, $P < 0.05$, $n = 8$), amylase (fourfold increase, $P < 0.01$, $n = 8$) and alanine aminotransferase (serum glutamic pyruvic transaminase; twofold increase, $P < 0.05$, $n = 8$) all indicative of cellular damage, high rates of cell death and cell turnover in tissue associated with the GI tract. At 10 weeks of age, hematoxylin and eosin (H and E) staining was performed, as previously described, which identified chronic mucosal damage with shortened and blunted villi in DKO mice compared with their WT littermates (Figures 5a and b, $*P < 0.001$, $n = 8$).¹⁰ These morphological changes could be attributed to the higher rates of apoptosis in the DKO mice compared with their WT littermates. The DKO mice also had a much higher frequency of goblet cells (Figures 5a and c; $*P < 0.01$, $n = 8$). The increase in the number of goblet cells in DKO mice may be an adaptive response to enhance the restorative function of the gut. This is consistent with the current thinking that goblet cells have a part in the protection rather than the pathogenesis of intestinal disorders.²⁴ It may be noted that a strong association between abnormal apoptosis, increased goblet cell numbers and GI disorders has been described previously.²⁵ Similar biochemical, morphological or histological changes were not noted in wild-type, villin or gelsolin single-knockout mice (Supplementary Figure 7A).

We also made the novel and unexpected observation that in the untreated DKO mice apoptotic cells appeared 'spontaneously' outside the crypts, all along the length of the villi (Figure 5d). Consistent with previous studies, we noted no apoptotic villus cells in the WT mice, under these conditions (Figure 5e).⁵ Furthermore, we noted that in WT mice, the apoptotic response to 8 Gy radiation (4 h) was greatest in epithelial cells located in the crypts (Figure 5e). Some apoptotic cells were seen in the lamina propria but none in the post-mitotic villus enterocytes of the WT mice. A significant increase in the number of apoptotic bodies was identified from H and E section of DKO mice treated with 8 Gy radiation (Figures 5e and f; $P < 0.01$ compared with WT littermates). Moreover, in the DKO mice apoptotic cells extended beyond the crypts, showing increased susceptibility of villus epithelial cells to γ -radiation-induced apoptosis (Figure 5g). In fact, apoptotic cells appeared at different positions all along the length of the villi of DKO mice treated with 8 Gy radiation (Figure 5h). As gelsolin is also expressed in dendritic cells, macrophages and vascular cells of the lamina propria, a slight increase in the number of apoptotic cells was noted in the lamina propria and submucosa of DKO mice compared with the WT littermates that was similar to that noted in gelsolin^{-/-} mice (Supplementary Figure 7B). There was no significant difference in the proliferation rates in the small bowel of WT and DKO mice (Supplementary Figure 8).

Transmission electron microscopy of the small bowel of 10-week-old DKO mice ($n = 8$) was performed on samples from proximal to distal ileum. Significant alterations in the microfilament structure were noted in the enterocytes of DKO mice compared with WT mice consistent with changes described previously in the villin^{-/-} and gelsolin^{-/-} knockout mice (data not shown).^{26,27} However, the most significant change that was noted only in the DKO mice was the presence of a large number of structurally abnormal mitochondria (Figure 6A) that were not seen in the WT, villin^{-/-} or gelsolin^{-/-} mice (Supplementary Figure 9). The majority of the mitochondria in DKO mice (78% $P < 0.001$, $n = 8$) showed evidence of damage, including complete loss or disorganization and collapse of cristae together with an accumulation of spherical, homogenous electron-dense lipid inclusions within the mitochondria (Figure 6B). This strong defect in the mitochondrial structure in the DKO mice correlates with the abnormal susceptibility of DKO villus cells to both spontaneous and γ -radiation-induced apoptotic cell death. The selective involvement of mitochondria in DKO mice confirmed the abnormal activation of apoptosis in these mice and indicated that villin and gelsolin function on an early step in the apoptotic signaling at the level of the mitochondria. Similar to gelsolin, villin targets to the mitochondria after the initiation of apoptosis (Figure 6C). Consequently, both proteins could regulate the initiation of apoptosis by altering mitochondrial dynamics.

Discussion

In the intestine, the expression of villin and gelsolin is highest in the 'apoptosis-resistant' villus cells and lowest in the 'apoptosis-sensitive' crypts.^{28,29} In this report, we demonstrate that the genetic deletion of villin and gelsolin activates abnormally high rates of apoptosis in villus epithelial cells that

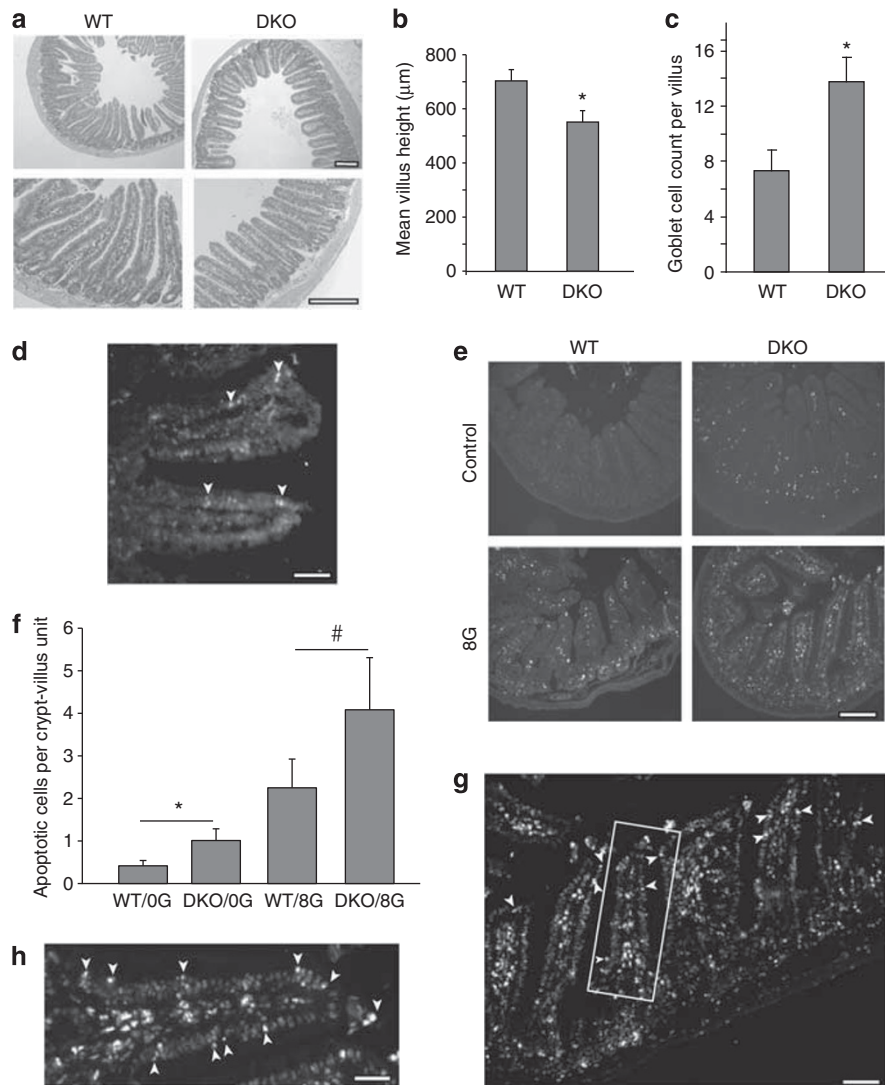


Figure 5 (a) Histological examination of H and E-stained ileum from WT and DKO mice. Bar, 500 μm . (b) DKO mice show blunted, shortened villi compared with WT mice ($P < 0.001$, $n = 8$). (c) DKO mice show a significant increase in the number of goblet cells. Goblet cells were counted in 20 full-length villi and crypts per mice and a total of eight WT and DKO mice were analyzed. The values obtained were averaged per villi and crypt for each tissue sample. Asterisk denotes statistically significant values compared with wild-type mice, $P < 0.01$. (d) Spontaneous apoptosis in the small intestine of DKO mice. Arrowheads point to apoptotic cells in villi of DKO mice identified by TUNEL assay. Data are from one representative experiment typical of eight other with similar results. Bar, 150 μm . (e) Control and irradiated small intestinal crypts and villi of WT and DKO mice (4 h after 8 Gy radiation) were analyzed for apoptotic cells. Apoptotic cells were defined using the TUNEL assay. Data are from one representative experiment typical of eight other with similar results. Bar, 400 μm . (f) The effects of 8 Gy irradiation on apoptosis in WT and DKO mice. Apoptotic cells were scored in 50, well-oriented crypt-villus units per section of the proximal half of the small intestine. At least three sections were analyzed per mouse. Control, non-irradiated DKO mice had more apoptotic cells than WT littermates ($*P < 0.05$, $n = 8$). γ -Irradiated-DKO mice had significantly more apoptotic cells compared with WT mice ($^{\#}P < 0.01$, $n = 8$). (g and h) Apoptotic villus cells in irradiated DKO mouse small intestine. Arrowheads indicate apoptotic cells identified by TUNEL assay. (h) A higher magnification of (g). Data are from one representative experiment typical of eight other with similar results. Bars, 200 μm (g) and 100 μm (h)

are otherwise extremely resistant to apoptotic cell death. Our study demonstrates that the regional differences in the expression of villin and gelsolin along the crypt-villus axis are mechanistically relevant and influence the apoptotic response of the GI epithelium. Although we have previously identified villin as a key regulator of apoptosis in the GI epithelium, we now show that the absence of both villin and gelsolin together is required to dissect the complex inter-relationship among all the apoptosis regulators relevant to the intestinal epithelium.¹⁰ Our findings provide a molecular basis for the regulation of normal GI homeostasis and indicate how

certain pathological responses could be generated in the GI epithelium by abnormal regulation of villin and gelsolin expression. Indeed, changes in villin expression are linked with several GI disorders associated with abnormal apoptosis.³⁰ Gelsolin levels are elevated in many senescent tissues where increased gelsolin expression is believed to be responsible for the resistance to apoptosis and to the increased susceptibility of these tissue to cancer.³¹

Studies done in yeast have shown that actin functions as a sensor that links changes in the nutritional status with mitochondrial-dependent commitment to cell death.³² A strong

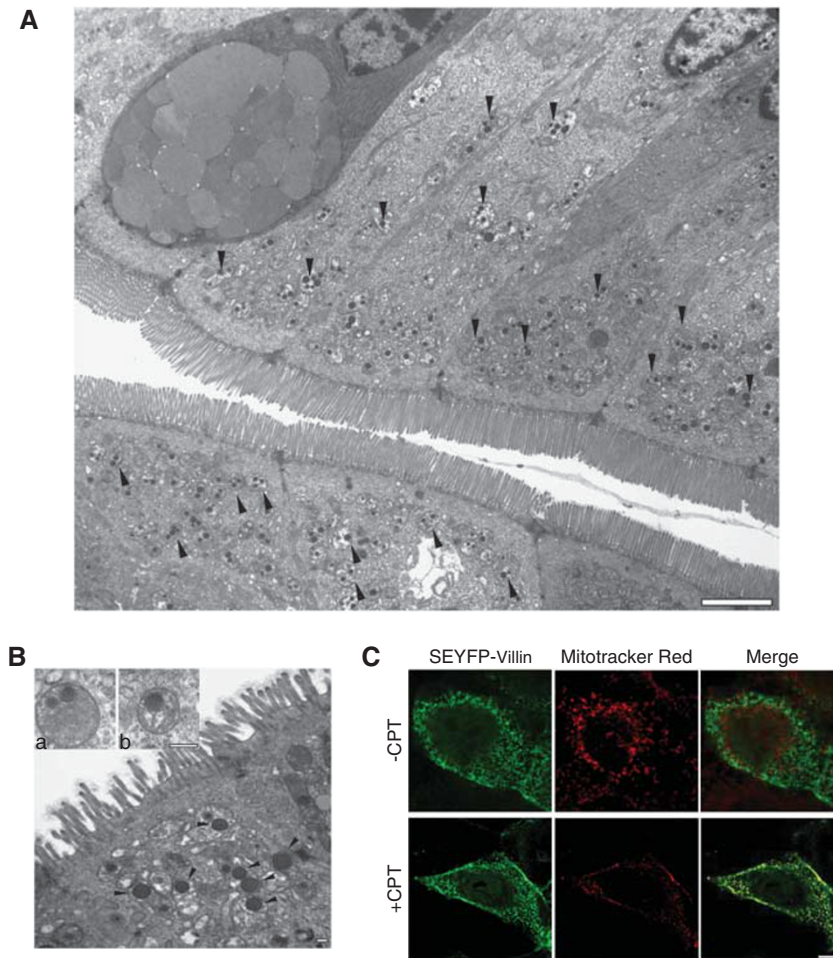


Figure 6 Ultrastructural analysis of small intestine of DKO mice shows abnormal mitochondria. **(A)** The majority of the villus cells in DKO mice have abnormal mitochondria (black arrowheads). Bar, 2 μm . **(B)** The mitochondria show complete loss, disorganization and collapse of cristae and accumulation of spherical homogenous electron-dense lipid inclusions (see inset) with the mitochondria (black arrowheads). Bars, 100 nm. Data are from one representative experiment typical of eight other with similar results. **(C)** Villin localizes to the mitochondria. MDCK Tet-Off cells stably transfected with super enhanced yellow fluorescent protein (SEYFP)-villin were stained with Mitotracker red (20 nM) and treated without or with CPT (20 μM). Co-localization of villin with mitochondria in CPT-treated cells is shown in the merged image. Bar, 5 μm

but as-yet-undefined link between the actin cytoskeleton and apoptosis has also been described in plant and animal cells.³² However, the precise mechanism by which the actin cytoskeleton regulates apoptosis in higher eukaryotes has remained largely uncharacterized. Furthermore, although several eukaryotic actin-regulatory proteins have been linked with cell survival, there are not too many studies that have examined the role of these proteins *in vivo*.³² Our study establishes a causal link between the actin cytoskeleton and apoptotic cell death in the GI epithelium. In this study we demonstrate that villin and gelsolin regulate cell survival by preserving steady state actin dynamics. Our studies also reveal that any global perturbation of the actin cytoskeleton are likely detrimental to cell survival. These findings are supported by our previous observation that a truncated mutant of villin (S1-S3) that severs actin in an unregulated manner induces apoptotic cell death.¹⁹ Similarly, a cleaved NH₂-terminal fragment (S1-S3) of gelsolin has been shown to enhance apoptosis.³³ More compelling data supporting our hypothesis comes from the observation that both, actin-binding

drugs that promote actin aggregation and actin-binding drugs that promote actin disruption, induce cell death and are currently being used as anti-cancer drugs.³⁴ This implicates regulated changes in the microfilament structure and the maintenance of a dynamic actin cytoskeleton in the preservation of cellular homeostasis and identifies actin-binding proteins as physiological regulators of apoptosis.

Similar to gelsolin, villin targets to the mitochondria, consequently, both proteins could regulate the initiation of apoptosis by altering mitochondrial dynamics. Apoptosis is initiated and regulated by changes in mitochondrial morphology and function mediated by changes in trafficking of anti- and pro-apoptotic proteins signals that in turn are regulated by their interaction with the microfilament structure.³⁵ How these protein signals are propagated is not known. As the actin cytoskeleton is a crucial component of the trafficking system, the transport of such cargo is likely influenced by the dynamic nature of the actin cytoskeleton. The ability of villin and gelsolin to associate with the actin cytoskeleton and the mitochondria suggests that they could regulate shuttling of

such cargo to or from the mitochondria. The mitochondria are the principal source of ATP and ATP levels are a crucial parameter of cellular homeostasis. It is estimated that a resting cell can consume as much as 50% of cellular ATP.³⁶ Remodeling of the microfilament structure involves hydrolysis of actin-bound ATP. Conserving ATP during cellular stress by modifying actin dynamics may therefore be a conserved mechanism for cell survival.

Materials and Methods

Materials. Monoclonal antibody for villin was purchased from ImmunoTech (Westbrook, ME, USA); polyclonal antibodies for gelsolin and villin were purchased from Santa Cruz (Santa Cruz, CA, USA). Phosphotyrosine antibody PY-20 was purchased from MP Biomedicals (Irvine, CA, USA). Ki67 antibody was purchased from AbCam (Cambridge, MA, USA). MDCK Tet-Off cells were a kind gift from KE Mostov (University of California-San Francisco, CA, USA). The villin knockout mice were a generous gift from D Gumucio (University of Michigan) and the gelsolin knockout mice were a kind gift from David Kwiatkowski (Harvard Medical School). QuikChange site-directed mutagenesis kit was purchased from Stratagene (La Jolla, CA, USA); GelCode Blue was from Pierce (Rockford, IL, USA). The caspase-3 substrate AC-DEVD-p-nitroanilide (pNA) was purchased from BIOMOL Research Laboratories (Plymouth Meeting, PA, USA). The *In situ* Cell Death Detection Kit was purchased from Roche (Mannheim, Germany). Cytochalasin D, Latrunculin B, Jasplakinolide and Hoechst 33258 were purchased from Sigma-Aldrich (St. Louis, MO, USA). MitoTracker Red was purchased from Invitrogen (Carlsbad, CA, USA).

Methods

Screening of DKO mice. The villin and gelsolin homozygous mice (villin^{-/-} and gelsolin^{-/-}) were crossed to generate the villin/gelsolin DKO. The genetic backgrounds and additional details, including changes in the microfilament organization in the villin^{-/-} and gelsolin^{-/-} mice are described elsewhere.^{26,27,37} Genotypes of DKO pups were determined by PCR as described previously, using a 5' primer, 5'-TGCCTGGCCTAAAGCTCAC-3' (Primer A) and two alternative 3' primers; 5'-ACCTGATCCTCCATATCTG-3' (primer B) that binds exon 1 sequence present only in villin wild-type allele and 5'-CGACAGTATCGGCTCAGG-3' (primer C) that binds within the LacZ gene of the targeted allele.³⁷ Primer set AB generated a 600-bp product (wild-type allele) and primer set AC produced a 900-bp fragment (targeted allele). The primers used for wild-type gelsolin allele were 5'-GGCCTGGTGAGAGAGTACTC-3' and 5'-CTTCTGCTCAGGTTCTGTCTG-3' and those for the gelsolin knock out allele (which bind the neomycin cassette) were, 5'-AGA GCAGCCGATTGCTGTG-3' and 5'-CTTCTGCTCAGGTTCTGTCTG-3'.²⁷ The first set of primers produced a 250-bp fragment and the latter set amplified a 200-bp fragment.

Cloning of wild-type and mutant villin proteins. Cloning in pTRE-HA of full-length human villin, PIP₂ binding site deletion mutants (Δ -PB1, -PB2 and -PB5), villin point mutant R138A; the substitution mutant (RKR) where arginine and lysine residues (¹³⁸R¹⁴⁵K¹⁴⁶R) in the villin PIP₂ binding domain PB2 were substituted with the neutral amino acid, alanine (¹³⁸A¹⁴⁵A¹⁴⁶A) and a villin mutant lacking all 10 identified tyrosine phosphorylation sites (VIL/AYFM) have been described in our previous studies.^{15,19,22}

Transfection of MDCK Tet-Off cells. MDCK Tet-Off cells were stably transfected with HA-tagged wild-type gelsolin, wild-type and mutant villin or super enhanced yellow fluorescent protein (SEYFP)-tagged full-length villin as described previously.¹⁹ Transfected cells were cultured in Dulbecco's modified Eagle's medium containing 100 μ g/ml G418 sulfate, 100 μ g/ml hygromycin B and 10% fetal bovine serum. To repress the expression of gelsolin and the wild-type and the mutant villin genes, cells were cultured in the presence of 10 ng/ml doxycycline.¹⁰ Doxycycline (10 ng/ml) treatment was used to suppress villin and gelsolin expression (VIL/NULL, GSN/NULL cells, respectively) and had no effect on actin levels. All studies were performed with single clones of MDCK cells expressing comparable levels of proteins. Additional studies were performed with a mixed population of clones, which provided similar results. All cell lines expressing either wild-type or mutant villin proteins cultured in the presence of doxycycline behaved similarly (data not shown).

Apoptosis assay. Apoptosis was induced by treating cells with CPT (20 μ M, 37 °C, 0–5 h) as described previously.¹⁰ The anti-apoptotic response of villin and gelsolin is not cell-type specific or determined by the type of apoptotic stimuli.¹⁰

Cell morphological analysis was done using bright-field images. Changes in nuclear morphology were identified using the cell-permeable DNA dye Hoechst 33258. Hoechst 33258 was added to the culture medium at a final concentration of 10 ng/ml for 10 min at 37 °C. All images were collected using a Nikon TE2000 fluorescence inverted microscope equipped with a CoolSnap FX charge-coupled device camera (Roper Scientific, Trenton, NJ, USA) and MetaMorph image analysis software 4.01 (Universal Imaging, Downingtown, PA, USA). To assess DNA cleavage PI was used as described elsewhere.¹⁰ The PI fluorescence intensity was measured using a LSR II Special Option Flow Cytometer (BD Biosciences, San Jose, CA, USA) equipped with an Enterprise II dual argon/UV laser. Data were recorded using FlowJo 7.1. software (Tree Star Inc., Ashland, OR, USA). A colorimetric protease assay was used to detect caspase-3 activity as described previously.¹⁰ Briefly, the assay is based on the spectrophotometric detection of the chromophore pNA after cleavage from the labeled substrate for caspase-3 (Ac-DEVD-pNA). The light emission of pNA was quantified using a microplate reader (Bio-Rad, Richmond, CA, USA) at 405 nm. Apoptosis was measured in villin^{-/-}, gelsolin^{-/-}, DKO and WT mice by counting TUNEL-positive nuclei, as well as histologically in H and E-stained sections of the small intestine essentially as described by us previously.¹⁰ TUNEL assay was performed on paraffin-embedded sections using an *in situ* cell death detection kit according to the manufacturer's instructions and as described by us previously.¹⁰ A negative control lacking the TUNEL reaction mixture was included in each assay. For these studies, latrunculin and jasplakinolide were used at concentrations that are not toxic to cells. Treatment of MDCK cells with jasplakinolide maintained F-actin filaments, whereas treatment of cells with latrunculin significantly decreased F-actin filaments in these cells.

Histology. For histological analysis, mice were killed and the small intestine was removed and fixed in 3.7% formalin. Paraffin-embedded sections of 5- μ m thickness were prepared and used for H and E staining. Villus height was measured as described previously.³⁸ For villin, gelsolin and Ki67 staining, tissue were deparaffinized in xylene for 10 min followed by incubation in serial dilutions of ethanol (100, 95 and 75%) for 5 min each. Following antigen retrieval, sections were incubated for 1 h at room temperature with anti-villin, anti-gelsolin or Ki67 antibodies. Negative controls included samples incubated without primary antibodies.

Electron microscopy. Mice were killed and the small intestine was fixed overnight in 2.5% glutaraldehyde prepared in 0.1 M sodium cacodylate buffer (pH 7.4). The tissue was post-fixed in 1% osmium tetroxide and dehydrated in a graded series of alcohol. The tissue samples were embedded in epon araldite and polymerized overnight in a 70 °C oven. The sections were cut using a Diatome diamond at 70–90 nm and stained with uranyl acetate and lead citrate. Images were collected on a JEOL 1200EX Electron microscope (JEOL USA, Peabody, MA, USA) with an AMT 2K digital camera.

Confocal microscopy. MDCK Tet-Off cells expressing full-length villin were cultured on coverslips in the absence or presence of doxycycline and treated with CPT (20 μ M, 0–5 h). Cells were fixed in 3.7% paraformaldehyde and permeabilized by incubation in phosphate-buffered saline (PBS) containing 0.1% Triton X-100. Cells were incubated with Alexa Fluor 488 (Invitrogen) phalloidin to record the distribution of F-actin. Fluorescence was recorded by confocal laser scanning microscopy (LSM 5 PASCAL; Carl Zeiss, Thornwood, NY, USA). MDCK Tet-Off cells stably transfected with SEYFP-villin cultured in chamber slides and treated without or with CPT were incubated with MitoTracker Red (100 nM, 45 min). Cells were washed and fixed with 3.7% formaldehyde. Fluorescence was recorded by confocal laser scanning microscopy (FV1000; Olympus, Center Valley, PA, USA). Images were processed with Metamorph 4.01.

Measurement of total cellular F-actin and G-actin content. Confluent cells were serum-starved overnight (1% serum) and apoptosis was induced by the addition of 20 μ M CPT for 0–5 h at 37 °C. Cells were fixed with 3.7% formaldehyde for 5 min and permeabilized for 1 min at 4 °C with 0.1% Triton X-100 in PBS, pH 7.4. To measure F-actin, cells were rinsed and incubated with 66 nM Alexa Fluor 488 phalloidin in PBS containing 1% BSA for 1 h at 37 °C. To measure G-actin, cells were treated and fixed as described above. However, cells were permeabilized with TBS (10 mM Tris and 0.15 M NaCl, pH 7.4) containing 0.1% Triton X-100, 2 mM MgCl₂, 0.2 mM DTT, and 10% glycerol (v/v) for 1 min at 4 °C. G-actin was labeled with 40 μ g/ml Alexa Fluor 488 DNase for 1 h at 37 °C. The total F-actin and G-actin content of cells was measured using the BD LSR II flow cytometer. Data were analyzed using FlowJo 7.1.

Visualization of free barbed ends. Cells were serum-starved overnight and treated with CPT (20 μ M, 0–5 h). Localization of free barbed ends was performed essentially as described before.^{39,40} Briefly, cells were fixed in 3.7% formaldehyde

and permeabilized for 1 min in the presence of 0.45 μ M Alexa Fluor 488-labelled G-actin in buffer containing 20 mM Hepes, pH 7.5, 138 mM KCl, 4 mM MgCl₂, 3 mM EGTA, 0.2 mg/ml saponin, 1 mM ATP and 1% BSA. Free barbed ends were measured using a confocal laser scanning microscope and a 63X oil objective (LSM 5 PASCAL; Carl Zeiss) at excitation and emission wavelengths of 488 and 505 nm respectively. Free barbed ends were quantified by measuring the average fluorescence intensity using Metamorph 4.01 software.

Conflict of Interest

The authors declare no conflict of interest.

Acknowledgements. This work was supported by National Institute of Diabetes and Digestive and Kidney Diseases grants DK-65006, DK-54755 and DK-81408 (to SK) and the Public Health Service grant DK56338.

- Hall PA, Coates PJ, Ansari B, Hopwood D. Regulation of cell number in the mammalian gastrointestinal tract: the importance of apoptosis. *J Cell Sci* 1994; **107** (Part 12): 3569–3577.
- Watson AJ. Apoptosis and colorectal cancer. *Gut* 2004; **53**: 1701–1709.
- Moss SF, Attia L, Scholes JV, Walters JR, Holt PR. Increased small intestinal apoptosis in coeliac disease. *Gut* 1996; **39**: 811–817.
- Fujise T, Iwakiri R, Wu B, Amemori S, Kakimoto T, Yokoyama F *et al*. Apoptotic pathway in the rat small intestinal mucosa is different between fasting and ischemia-reperfusion. *Am J Physiol Gastrointest Liver Physiol* 2006; **291**: G110–G116.
- Potten CS. The significance of spontaneous and induced apoptosis in the gastrointestinal tract of mice. *Cancer Metastasis Rev* 1992; **11**: 179–195.
- Keefe DM, Brealey J, Goland GJ, Cummins AG. Chemotherapy for cancer causes apoptosis that precedes hypoplasia in crypts of the small intestine in humans. *Gut* 2000; **47**: 632–637.
- Potten CS, Merritt A, Hickman J, Hall P, Faranda A. Characterization of radiation-induced apoptosis in the small intestine and its biological implications. *Int J Radiat Biol* 1994; **65**: 71–78.
- Khurana S. Structure and function of villin In: Bittar EE (series ed), Khurana S (volume ed), *Advances in Molecular and Cell Biology*, 37. *Aspects of the Cytoskeleton*, chapter 5, vol. 37. Elsevier: San Diego, CA, 2006, pp 89–117.
- Yin HL, Albrecht JH, Fattoum A. Identification of gelsolin, a Ca²⁺-dependent regulatory protein of actin gel-sol transformation, and its intracellular distribution in a variety of cells and tissues. *J Cell Biol* 1981; **91** (3 Part 1): 901–906.
- Wang Y, Srinivasan K, Siddiqui MR, George SP, Tomar A, Khurana S. A novel role for villin in intestinal epithelial cell survival and homeostasis. *J Biol Chem* 2008; **283**: 9454–9464.
- Gourlay CW, Ayscough KR. The actin cytoskeleton: a key regulator of apoptosis and ageing? *Nat Rev Mol Cell Biol* 2005; **6**: 583–589.
- Friederich E, Huet C, Arpin M, Louvard D. Villin induces microvilli growth and actin redistribution in transfected fibroblasts. *Cell* 1989; **59**: 461–475.
- Posey SC, Bierer BE. Actin stabilization by jasplakinolide enhances apoptosis induced by cytokine deprivation. *J Biol Chem* 1999; **274**: 4259–4265.
- Azuma T, Kohts K, Flanagan L, Kwiatkowski D. Gelsolin in complex with phosphatidylinositol 4,5-bisphosphate inhibits caspase-3 and -9 to retard apoptotic progression. *J Biol Chem* 2000; **275**: 3761–3766.
- Kumar N, Zhao P, Tomar A, Galea CA, Khurana S. Association of villin with phosphatidylinositol 4,5-bisphosphate regulates the actin cytoskeleton. *J Biol Chem* 2004; **279**: 3096–3110.
- de Arruda MV, Bazzari H, Wallek M, Matsudaira P. An actin footprint on villin. Single site substitutions in a cluster of basic residues inhibit the actin severing but not capping activity of villin. *J Biol Chem* 1992; **267**: 13079–13085.
- Andre E, Lottspeich F, Schleicher M, Noegel A. Severin, gelsolin, and villin share a homologous sequence in regions presumed to contain F-actin severing domains. *J Biol Chem* 1988; **263**: 722–727.
- Zhai L, Zhao P, Panebra A, Guerrero AL, Khurana S. Tyrosine phosphorylation of villin regulates the organization of the actin cytoskeleton. *J Biol Chem* 2001; **276**: 36163–36167.
- Tomar A, George S, Kansal P, Wang Y, Khurana S. Interaction of phospholipase C-gamma1 with villin regulates epithelial cell migration. *J Biol Chem* 2006; **281**: 31972–31986.
- Mathew S, George SP, Wang Y, Siddiqui MR, Srinivasan K, Tan L *et al*. Potential molecular mechanism for c-Src kinase mediated regulation of intestinal cell migration. *J Biol Chem* 2008; **283**: 22709–22722.
- De Corte V, Gettemans J, Vandekerckhove J. Phosphatidylinositol 4,5-bisphosphate specifically stimulates PP60(c-src) catalyzed phosphorylation of gelsolin and related actin-binding proteins. *FEBS Lett* 1997; **401**: 191–196.
- Tomar A, Wang Y, Kumar N, George S, Ceacareanu B, Hassid A *et al*. Regulation of cell motility by tyrosine phosphorylated villin. *Mol Biol Cell* 2004; **15**: 4807–4817.
- Mathew S, George SP, Wang Y, Siddiqui MR, Srinivasan K, Tan L *et al*. Potential molecular mechanism for c-Src kinase-mediated regulation of intestinal cell migration. *J Biol Chem* 2008; **283**: 22709–22722.
- Itoh H, Beck PL, Inoue N, Xavier R, Podolsky DK. A paradoxical reduction in susceptibility to colonic injury upon targeted transgenic ablation of goblet cells. *J Clin Invest* 1999; **104**: 1539–1547.
- Reuter BK, Pizarro TT. Mechanisms of tight junction dysregulation in the SAMP1/YitFc model of Crohn's disease-like ileitis. *Ann NY Acad Sci* 2009; **1165**: 301–307.
- Ferrary E, Cohen-Tannoudji M, Pehau-Arnudet G, Lapillonne A, Athman R, Ruiz T *et al*. *In vivo*, villin is required for Ca(2+)-dependent F-actin disruption in intestinal brush borders. *J Cell Biol* 1999; **146**: 819–830.
- Witke W, Sharpe AH, Hartwig JH, Azuma T, Stossel TP, Kwiatkowski DJ. Hemostatic, inflammatory, and fibroblast responses are blunted in mice lacking gelsolin. *Cell* 1995; **81**: 41–51.
- Dudouet B, Robine S, Huet C, Sahuquillo-Merino C, Blair L, Coudrier E *et al*. Changes in villin synthesis and subcellular distribution during intestinal differentiation of HT29-18 clones. *J Cell Biol* 1987; **105**: 359–369.
- Lueck A, Brown D, Kwiatkowski DJ. The actin-binding proteins adseverin and gelsolin are both highly expressed but differentially localized in kidney and intestine. *J Cell Sci* 1998; **111** (Part 24): 3633–3643.
- Simms LA, Doecke JD, Walsh MD, Huang N, Fowler EV, Radford-Smith GL. Reduced alpha-defensin expression is associated with inflammation and not NOD2 mutation status in ileal Crohn's disease. *Gut* 2008; **57**: 903–910.
- Ahn JS, Jang IS, Kim DI, Cho KA, Park YH, Kim K *et al*. Aging-associated increase of gelsolin for apoptosis resistance. *Biochem Biophys Res Commun* 2003; **312**: 1335–1341.
- Franklin-Tong VE, Gourlay CW. A role for actin in regulating apoptosis/programmed cell death: evidence spanning yeast, plants and animals. *Biochem J* 2008; **413**: 389–404.
- Kothakota S, Azuma T, Reinhard C, Klippel A, Tang J, Chu K *et al*. Caspase-3-generated fragment of gelsolin: effector of morphological change in apoptosis. *Science* 1997; **278**: 294–298.
- Algeciras-Schimmich A, Pietras EM, Barnhart BC, Legembre P, Vijayan S, Holbeck SL *et al*. Two CD95 tumor classes with different sensitivities to antitumor drugs. *Proc Natl Acad Sci USA* 2003; **100**: 11445–11450.
- Puthalakath H, Villunger A, O'Reilly LA, Beaumont JG, Coultas L, Cheney RE *et al*. Bmf: a proapoptotic BH3-only protein regulated by interaction with the myosin V actin motor complex, activated by anoikis. *Science* 2001; **293**: 1829–1832.
- Bernstein BW, Bamberg JR. Actin-ATP hydrolysis is a major energy drain for neurons. *J Neurosci* 2003; **23**: 1–6.
- Pinson KI, Dunbar L, Samuelson L, Gumucio DL. Targeted disruption of the mouse villin gene does not impair the morphogenesis of microvilli. *Dev Dyn* 1998; **211**: 109–121.
- Ohneda K, Ulshen MH, Fuller CR, D'Ercole AJ, Lund PK. Enhanced growth of small bowel in transgenic mice expressing human insulin-like growth factor I. *Gastroenterology* 1997; **112**: 444–454.
- Chan AY, Raft S, Bailly M, Wyckoff JB, Segall JE, Condeelis JS. EGF stimulates an increase in actin nucleation and filament number at the leading edge of the lamellipod in mammary adenocarcinoma cells. *J Cell Sci* 1998; **111** (Part 2): 199–211.
- Athman R, Louvard D, Robine S. Villin enhances hepatocyte growth factor-induced actin cytoskeleton remodeling in epithelial cells. *Mol Biol Cell* 2003; **14**: 4641–4653.

Supplementary Information accompanies the paper on Cell Death and Differentiation website (<http://www.nature.com/cdd>)